Transactions **of the SMiRT 27**
Yokohama, Japan, March 3-8, 2024
Division XII

Investigations of additively manufactured 22NiMoCr3-7 reactor steel using Charpy V-notch testing

Linda Mally[1], Michael Seidenfuß[2], Stefan Weihe[2]

[1]M.Sc., Institute for Materials Testing, Materials Science and Strength of Materials (IMWF) University of Stuttgart, Stuttgart, Germany (linda.mally@imwf.uni-stuttgart.de)
[2]Prof. Dr.-Ing., Institute for Materials Testing, Materials Science and Strength of Materials (IMWF) University of Stuttgart, Stuttgart, Germany

ABSTRACT

This study is based on the detection and analysis of crack-like anomalies in the ferritic reactor pressure vessels (RPV) found at Doel 3 and Tihange 2 nuclear power stations. Discovered during routine ultrasonic testing in 2012, these anomalies were identified as hydrogen flakes, formed during vessel manufacturing. These flakes varied in size and orientation, posing a challenge to the assessment of the structural integrity of the vessels. Current standards for evaluating such defects were found inadequate, as they did not fully account for the mixed-mode loading conditions experienced by the RPVs. Ongoing research projects at MPA University of Stuttgart aim to address this gap by improving fracture mechanics-based evaluation methods. This involves new experimental and numerical simulations using damage mechanics, with a focus on establishing new interaction criteria for various stress and strain conditions. A novel approach is being pursued that uses additive manufacturing to produce specimens with internal crack patches that realistically replicate the detected defects into a physical twin that can be easily tested and analyzed. For this study the ferritic-bainitic reactor steel 22NiMoCr3-7 (similar to ASTM A 508 Cl.2) was used. The processability of this material via laser powder bed fusion (L-PBF) was confirmed. It was demonstrated that the additively manufactured material followed by heat treatment, exhibits comparable properties (tensile strength, hardness, elongation, microstructure) to the forged reference material, essential for the accuracy and the transferability of the results. This approach, employing a physical twin, allows for more accurate assessments of structural integrity and failure mechanisms. The work presented here focuses on a comprehensive material characterization, including Charpy impact testing, to evaluate the anisotropy and ductile-to-brittle transition temperature of the material. These efforts are instrumental in advancing the understanding of ferritic materials in additive manufacturing and their applications in nuclear reactor components. As expected the Charpy impact energy is highest for specimens with a 0° orientation (corresponds to exposure plane) and decreases as the angle of the build-up direction increases. The impact strength of standing specimens (90° build-up direction) is the lowest. The results confirm the expectations that 90° is the most critical build-up direction, as the crack propagates between the individual melted layers. The results of the Charpy impact tests show unexpected little scatter in the transition area, but significant scatter in the upper shelf temperature. The scatter is lowest at a build-up direction of 0° and highest at 90°. This raises the question of whether it is generally sufficient to fully examine and evaluate only the most critical build-up direction for additively manufactured components.

INTRODUCTION

Numerous crack-like anomalies were detected during routine ultrasonic testing in the walls of the ferritic reactor pressure vessels (RPV) at Doel 3 and Tihange 2 nuclear power stations in Belgium in 2012. Further analysis concluded that the anomalies were hydrogen flakes, formed during the manufacturing process of the vessels. These flakes were found along segregation lines and exhibited an inclination ranging from 0° (indicating a laminar orientation) to 16° (suggesting a quasi-laminar orientation) in relation to the vessel's pressure-retaining surface. Their sizes varied from a few millimeters to several centimeters [Doel 3 (2012),

Tihange 2 (2012)]. Current standards and guidelines [ASME (2015), ASME (2016), FKM (2009)] employ interaction criteria and substitution methods for the safety assessment of the structural integrity of pressurized components with multiple defects. These interaction criteria are based on linear-elastic fracture mechanic and experiments based on pure mode I stress conditions [Lacroix et al. (2015)]. In reality, the found crack fields are subjected to mixed-mode loading with the primary loading direction being along the plane of crack (Mode II), because of the crack alignment parallel to the vessel wall. Methods for the evaluation of single cracks loaded in mixed mode are known, but are not very well validated. The research project MeKom II [BMUV-Research project 1501596A] at the Materials Testing Institute at the University of Stuttgart (MPA) aims to validate and improve the existing fracture mechanics-based evaluation methods by conducting new experimental approaches and numerical simulations using damage mechanics. The project also intends to establish interaction criteria based on damage mechanics to predict local plastic deformation and the failure mechanisms under various geometric, stress, and strain conditions [Beremin (1983), Rousselier (1987), Seidenfuß et al. (2014)]. Specimens with internal crack fields which have previously been detected using non-destructive testing methods are required to provide a realistic assessment. Internal defects with a specified position, size and geometry can only by created using additive manufacturing. These crack fields are incorporated in a physical twin (geometrically scaled specimen or model) and tested under specific loading and deformation scenarios in order to test structural integrity and predict the time of failure. Prerequisite for the successful use of a physical twin: The material behavior of the additive material must be sufficiently close to the original part (reference material) in order to rule out errors in the transferability of the results. In the context of MeKom II the processability of the ferritic-bainitic reactor steel 22NiMoCr3-7 was confirmed using laser powder bed fusion (L-PBF). It was shown that the material behaviour (microstructure, hardness and tensile strength) of the additive material followed by a heat treatment has comparable properties to that of the forged reference material [Mally (2022), Stumpfrock (2022)].

This work contributes to the comprehensive material characterization of the additively processed ferritic-bainitic reactor steel 22NiMoCr3-7. Current guidelines and standards for additive manufacturing recommend that the material properties listed in the conventional material standard are also declared for the corresponding additively manufactured materials [VDI 3405 Sheet 2.6]. Depending on the area of application, further specific material properties should be investigated. The OSKO project [BMUV - research project 1501644] was launched to conduct an in-depth material characterization and to investigate the correlations of the resulting material behaviour with the additive manufacturing process. This also includes Charpy impact testing. Charpy impact tests play an integral role in the material qualification process of new alloys for additive manufacturing, helping to quickly assess the suitability of new materials and the used process parameters for AM processes [Beckers (2019)]. While strength and elongation (from the tensile testing) can provide quite satisfactory results, defects resulting from the manufacturing process (including pores) often only manifest themselves in a decrease of notch impact energy [Ty (2023)].

Ferritic materials are rarely researched for the application in additive manufacturing processes like L-PBF [Jiang (2021)]. Current literature focuses mostly on aluminum, titanium or nickel-based alloys. Because of recent advances in additive manufacturing, AM is considered a new possible manufacturing method for advanced reactor components, therefore making ferritic materials interesting candidate materials [Sridharan (2019)]. According to different guidelines, e.g. KTA 3201.1, which describes the requirement for ferritic materials for components of the primary circuit of light water reactor concepts, the impact energy at low and high temperatures must be investigated using Charpy impact testing to determine the ductile-to-brittle transition temperature and the brittle fracture resistance.

In this study, Charpy impact tests are performed and the results compared with the mechanical properties of the forged reference material. Due to the process-related anisotropy of certain material properties, Charpy impact specimens are produced and tested in several build-up directions as recommended in VDI 3405 Sheet 2.6. The quality of the individual build-up directions and the suitability

of the process parameters used are evaluated. By comparing the build-up directions, the strength of the anisotropy of the material properties is quantified and the critical build-up direction is determined. In addition, the impact energy at low and high temperatures (lower and upper shelf temperature) is investigated and the ductile to brittle transition temperature is determined. Together with the previous investigations of the material properties, this work forms the basis for the upcoming fracture mechanics investigations.

EXPERIMENTAL METHODOLOGY

Material

For this study the reactor steel 22NiMoCr3-7 (similar to ASTM A 508 Cl.2) which is a hypoeutectoid steel with a carbon content of approx. 0.22%, to which nickel, molybdenum and chromium are alloyed, is used. The material was atomized by Höganäs by means of Vacuum induction melting Inert Gas Atomization (VIGA) using nitrogen. The specified limit values for this material are based on the acceptance test from TÜV Bayern [TÜV (1976)]. They are displayed in Table 1 together with the results of the conducted element analysis by Höganäs. These test results confirm that the chemical composition of the powder is still within the specified range and allows a later comparison between the additive manufactured material and the conventionally manufactured (forged) reference material.

Table 1 - 22NiMoCr3-7 specification and chemical composition

	Fe	**C**	**Si**	**Mn**	**P**	**S**	**Cu**	**Sn**	**Al**
Spec. min.	Balance	0.17	0.10	0.50	-	-	-	-	-
Spec. max.	Balance	0.25	0.35	1.00	0.012	0.015	0.1	-	0.05
Powder	Balance	0.19	0.22	0.93	0.006	0.004	0.007	0.02	0.02
	Cr	**Mo**	**Ni**	**V**	**Ta**	**Co**	**As**	**Sb**	
Spec. min.	0.25	0.50	0.60	-	-	-	-	-	
Spec. max.	0.50	0.75	1.00	0.050	0.030	0.030	-	-	
Powder	0.28	0.51	0.67	< 0.01	< 0.01	0.01	-	-	

Laser powder bed fusion of 22NiMoCr3-7

A SLaVAM 300 L-PBF system from Evobeam was used to produce all specimens. The system is equipped with a 2kW single mode Ytterbium fiber laser with a wavelength of $\lambda = 1075 \pm 7$ nm. The specimens were printed using the optimal process parameter sets previously determined in a parameter study, namely a laser power of 400 W, a scanning speed of 1200 mm/s, spot diameter 62 µm, 30 µm layer thickness and 150 °C build chamber temperature. A multi-directional stripe scan strategy with a hatch distance of 100 µm, a stripe overlap of 100 µm and layer rotation of 67° was used for all specimens.

Due to the physics of the additive manufacturing process, AM parts exhibit material properties that may be both location specific and anisotropic. Specimen fabrication is for this reason carried out in three build-up directions (0°, 45° and 90°), multiple build jobs and different locations on the build plate. All specimens are printed as blanks, heat treated and then machined to specimen shape.

Post processing – heat treatment and specimen fabrication

The rapid cooling rate during the additive manufacturing process results in a fine-grained martensitic microstructure. In order to achieve the required target microstructure (ferritic-bainitic microstructure with fine to slightly coarse grain size) a subsequent heat treatment is necessary. Therefore, all specimens are subjected to the following heat treatment which yielded in the strongest similarity in terms of microstructure

and mechanical properties to the conventionally manufactured reference material: Austenitized for one hour at 900 °C and then cooled slowly to 100 °C in an oven and then tempered at 700 °C for 480 minutes and cooled in air [Mally (2022)]. After heat treatment all specimen blanks were machined to the standard size of V-notched Charpy specimens (10 mm x 10 mm x 55 mm) in accordance with DIN EN ISO 148-1:2017-05. The V-notch is located on the upper surface of all samples, i.e. opposite the holder that was additionally printed for simplified mechanical post-processing, see Figure 1.

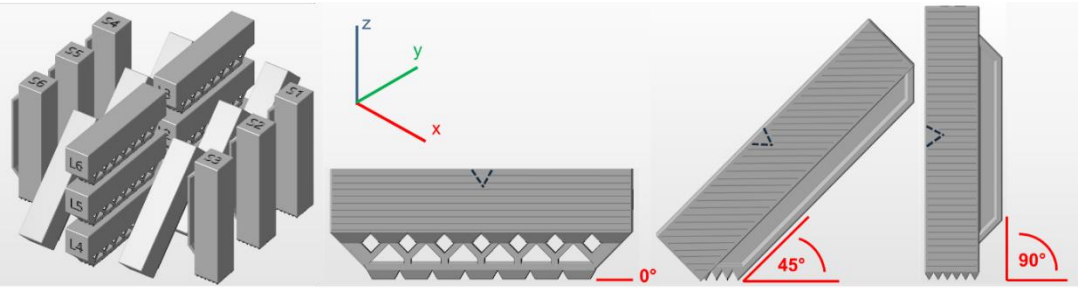

Figure 1 – Build-up directions and position during manufacturing

Mechanical property characterization

Charpy impact tests were carried out in accordance with DIN EN ISO 148-1 in a temperature range of -150 °C to 150 °C on a 300 J notched bar impact bending machine from Roell & Korthaus-Amsler. After Charpy impact testing, the fracture surfaces (shear fracture percentage), the impact energy and the lateral expansion were evaluated for all samples. The fracture surfaces were investigated using a Hitachi TM4000 scanning electron microscope. Microstructural investigations (microstructure, defects and porosity) were carried out on metallographic sections cut out perpendicularly to the fracture surface using a Leica DM 8000 M optical microscope.

In addition, the transition temperature from Charpy impact testing was determined using the following criteria specified in the DIN EN ISO 148-1 standard:

- T_{t27} the temperature when the impact energy of 27 J is reached
- $T_{t0.9}$ is the temperature at which the specimen broadens laterally by 0.9 mm and
- $T_{t50\%SFA}$ the temperature at which 50% ductile content occurs on the fracture surface.

RESULTS AND DISCUSSION

The impact energy, the lateral expansion and the shear fracture percentage are evaluated separately for each build-up direction and plotted in Figure 2-4. The fracture surfaces for the lower shelf temperature, transition temperature and upper shelf temperature are also shown in the corresponding figures. The approximation curves are based on mathematical functions describing the results from Charpy impact tests [Hofer (1997)]. The transition temperature for each build-up direction is determined using the above-mentioned criteria and are shown in Table 2.

Table 2: Transition temperatures determined using Charpy impact tests

Orientation	0°	45°	90°	Reference material
Impact energy T_{27} [°C]	-58.7	-41.5	-29.6	-51.6
Widening $T_{0.9}$ [°C]	-47.8	-31.7	-6.8	/
Shear fracture percentage $FATT_{50}$ [°C]	-8.9	-1.8	15.7	/

0° specimens

Based on the current test results (see Figure 2) it can be concluded that the lower shelf temperature range starts between -60 °C and -100 °C. At -100 °C complete cleavage fracture is observed. The onset of the upper shelf temperature range is at approx. 40 °C. A maximum impact energy of 199 J is achieved at 60° C. At 60 °C a few specimens start showing 100% shear fracture, which corresponds to complete ductility of the material.

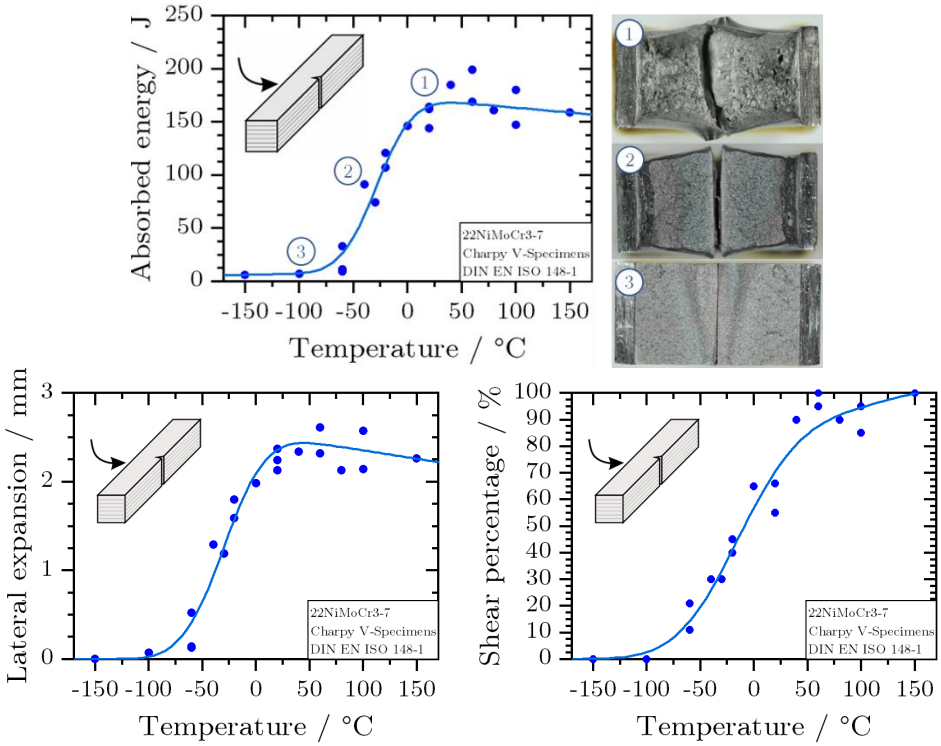

Figure 2 - Visualization of Charpy Impact results for the 0° specimens incl. approximation curves

The SEM images (Figure 3) of the fracture surfaces for the 0° specimens show complete brittle fracture at -100 °C. No major pores or bonding defects could be detected. The fracture surface at room temperature (RT), 20 °C, shows complete ductile fracture. Several cavities with freely solidified surfaces ("dimples") can be seen, which can be clearly distinguished from the surrounding fine honeycomb structure. The majority of these dimples range between 10 to 60 µm in size, with a few reaching up to 100 µm. The size of the dimples of up to approx. 50 µm suggests that they are most likely gas pores from the manufacturing process. Compared to the sample at RT, the number of imperfections on the fracture surface of the specimen tested at 60 °C has increased while the size of the imperfections appears to be unchanged.

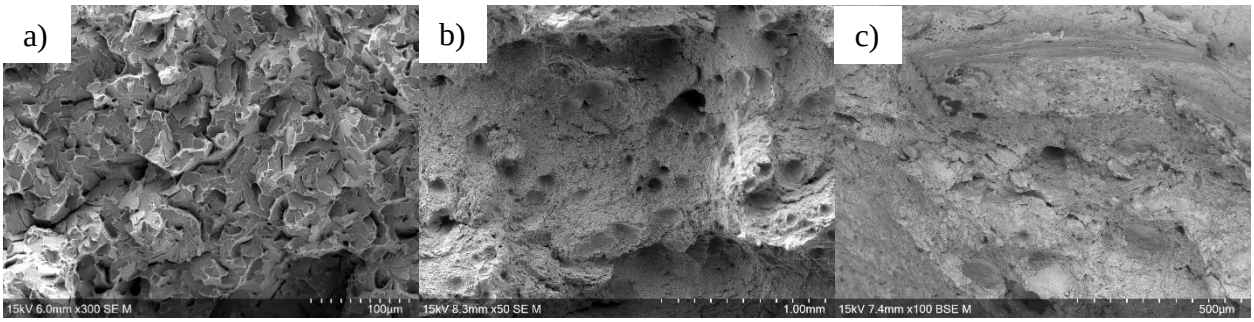

Figure 3 – SEM imaging of fracture surface of the 0° specimen at -100 °C (a), 20 °C (b) and 60 °C (c)

45° specimens

Again, the lower shelf temperature range begins between -60 °C to -100 °C, while the upper shelf temperature starts at approx. 40 °C. Scattering in the upper temperature range is noticeable. A maximum impact energy of 175 J is achieved at 20 °C. As with the 0° specimens, 100% shear fracture can be observed in some specimens starting at over 60° (Figure 4).

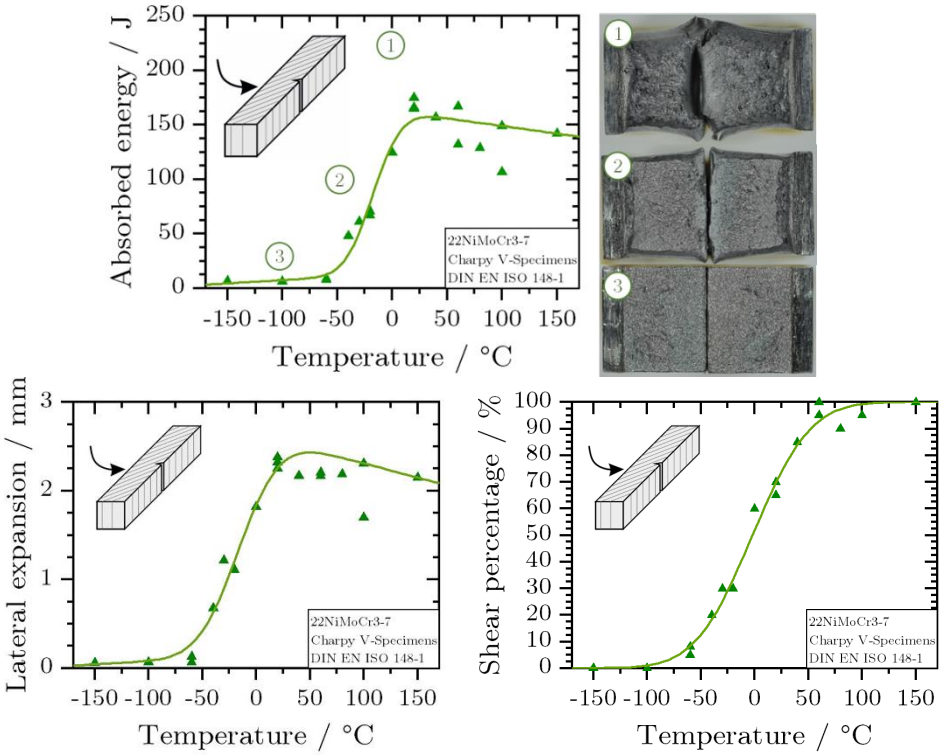

Figure 4 - Visualization of Charpy Impact results for the 45° specimens incl. approximation curves

The SEM images (Figure 5) of the fracture surfaces for the 45° specimens also show complete brittle fracture at -100 °C. No particular anomalies were detected. At room temperature (RT), 20 °C, the fracture surface shows full ductile fracture. The fracture surface is similar to that of the 0° specimens. The described dimples are also visible here. However, unmelted powder particles could be detected in some of these defects. The size of the dimples here also varies 10 to 60 µm in size, with a few bigger ones reaching 100 µm. Compared to the sample at RT, the number of imperfections on the fracture surface of the specimen tested at 60 °C has slightly increased while the size of the imperfections appears to be unchanged.

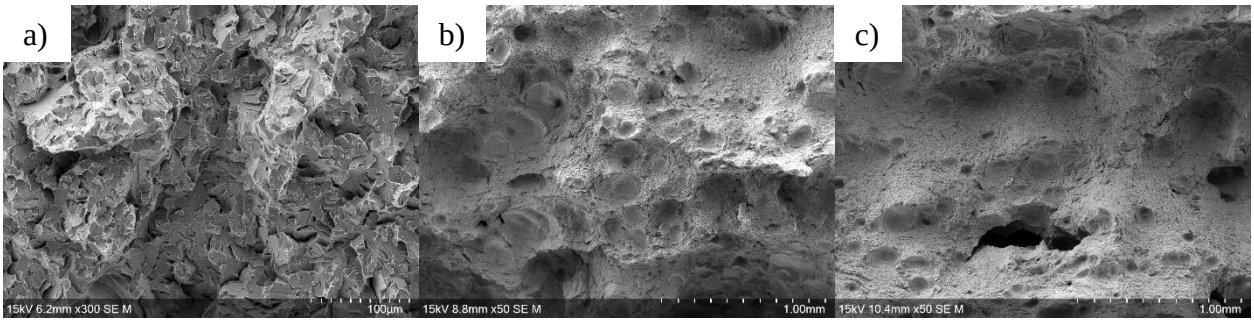

Figure 5 – SEM imaging of fracture surface of the 45° specimen at -100 °C (a), 20 °C (b) and 60 °C (c)

90° specimens

Just as with the other build-up directions, the lower shelf temperature of the 90° specimens starts between -60 °C and -100°C, with the upper shelf temperature onset at approx. 40 °C. Looking at the impact energy significant scatter in the upper temperature range can be seen. A maximum impact energy of 134 J is achieved at 20 °C. Like with the 0° and 45° specimens 100% shear fracture can be observed beginning at over 60° (Figure 6).

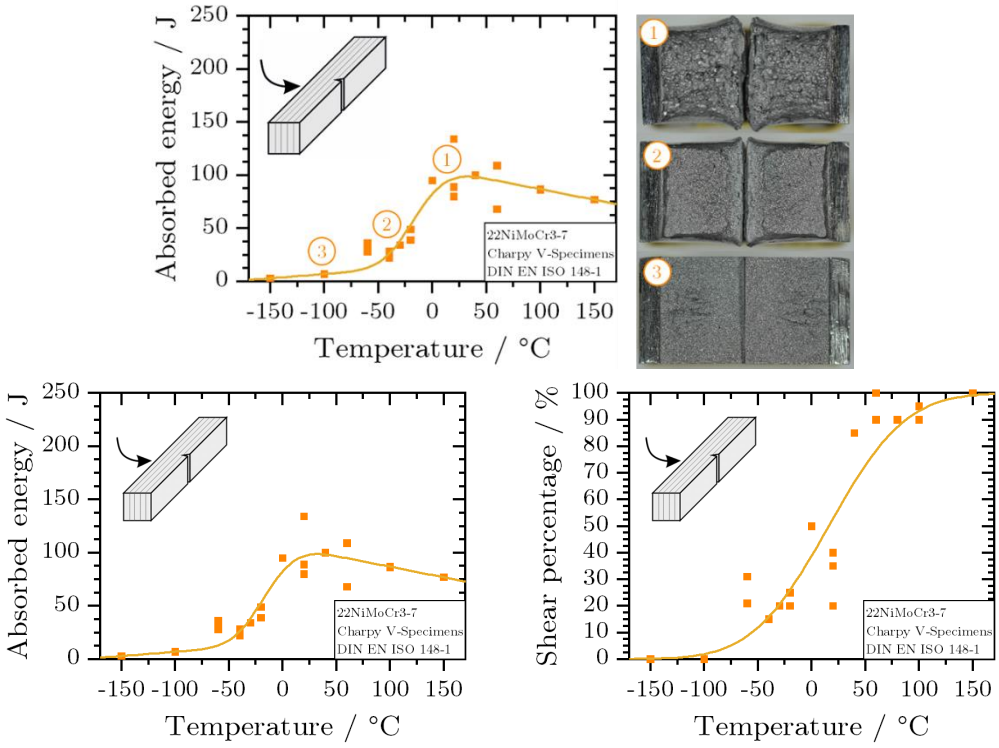

Figure 6 - Visualization of Charpy Impact results for the 90° specimens incl. approximation curves

The SEM images (Figure 7) of the fracture surfaces for the 90° specimens also show complete brittle fracture at -100 °C. No particular anomalies were detected. At room temperature (RT), 20 °C, mostly ductile fracture but with smaller areas of brittle fracture is displayed (see Figure 7b). Compared to the 0° and 45° specimens, the number of imperfections increased further. These make up the majority of the fracture surface. The dimple size remains unchanged (approx. 10 - 60 µm). Compared to the 45° sample, the number of unfused powder particles in the dimples increased further.

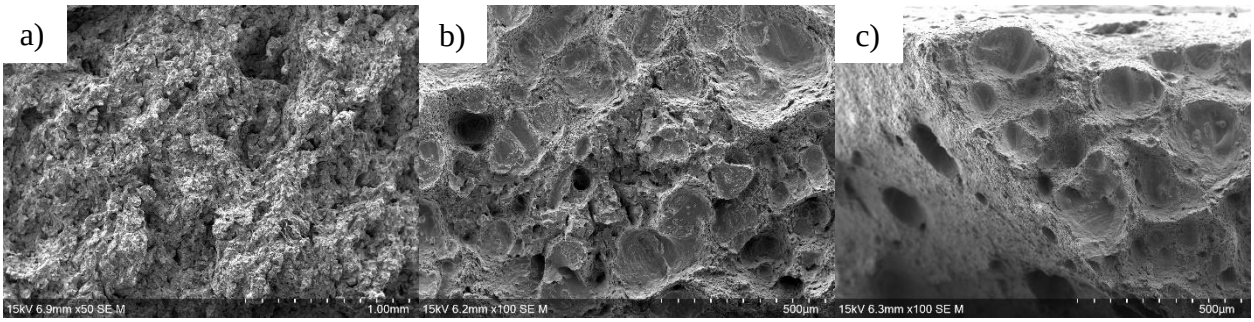

Figure 7 – SEM imaging of fracture surface of the 90° specimen at -100 °C (a), 20 °C (b) and 60 °C (c)

Evaluation and comparison to the reference material

In Figure 8 the approximation curves of all three build-up directions are plotted together with the approximation curve of the forged reference material. The database of the reference material is based on material extracted at T/2 in T-S direction. Comparing the approximation curves of the additively manufactured specimens with those of the reference material (red curve), it is noticeable that the curve of the 0° specimens (blue curve) is the most similar to that of the reference material. The upper shelf temperature of the 0° specimens shows only a minimal deviation from the reference material. A marginal downward trend in the impact energy can be recognized for the 0° specimen. The biggest difference to the reference material is that the curve of the 0° specimens is shifted towards lower temperatures. As the curve for the 0° specimens is shifted to the lower temperature range, this could indicate a reduced stress multi-axiality.

The results of the 45° specimens (green curve) correspond exactly to the curve of the reference material in the lower shelf area. Only a very slight deviation of the curves is visible in the transition area. The greatest difference to the reference material can be seen in the upper shelf temperature range. Overall, the 45° specimens reach lower impact energies there. In addition, a drop in the curve with increasing temperature can be seen in this area.

The impact energy achieved by the 90° specimens (orange curve) is the lowest compared to the other additively manufactured specimens. Although the approximation curve agrees very well with that of the reference material in the low-temperature range, there is a significant drop in the impact energy achieved from room temperature to higher temperatures.

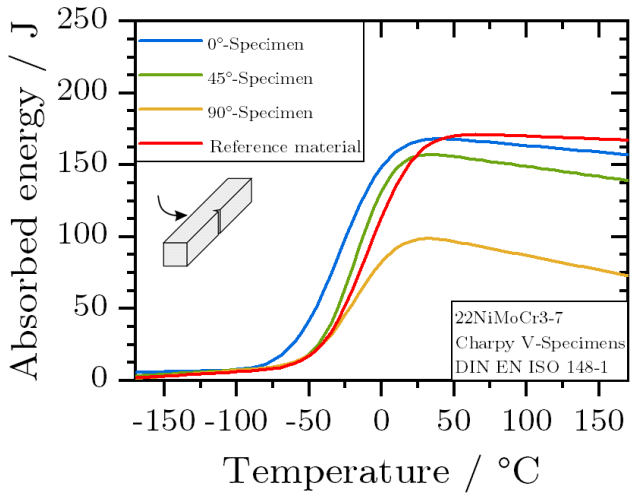

Figure 8 - Comparison between reference material and additive manufactured material

CONCLUSION

The evaluation of the Charpy impact energy for the three different build-up directions shows that the Charpy impact strength is highest for samples with a 0° orientation and decreases as the angle of the build-up direction increases. The impact energy of standing specimens (90° build-up direction) is the lowest. This behaviour was observed for all samples in the tested temperature range between -150 °C and 150 °C. Contrary to expectations, the scatter of the measured values is minimal in the transition area. However, there is significant scatter in the upper temperature range. The results of the Charpy impact tests show that the scatter of the measured values is also related to the build-up angle. The scatter of the measured values

likewise increases with increasing build-up angle. Overall the results confirm the expectations that 90° is the most critical build-up direction, because the fracture plane is parallel to the building plane resulting in crack propagation between the individual melted layers. This raises the question of whether it is generally sufficient for additively manufactured components to fully examine and evaluate only the most critical build-up direction.

The origin of the dimples on the fracture surfaces has not yet been established. An evaluation of the position of the samples during manufacturing shows no correlation between the position and the sample quality. The fact that more unmelted powder particles could be detected as the build-up angle increased suggests that the set of manufacturing parameters used may not deliver equally good results for all build-up directions and increases the amount of anisotropy. One reason for this may be the different cross-sectional areas (exposure area per layer) of the various specimens, which has a significant influence on heat dissipation.

OUTLOOK

The current results show that the processability of the material with the L-PBF process is not entirely independent of the geometry and that there is still considerable potential for further development.

As a basis for the following fracture mechanics tests, instead of using Pellini specimens, the reference temperature for all three different build-up directions of the additive material is estimated on instrumented Charpy impact specimens using the T4kN criterion.

Metallographic sections of the tested specimens are being prepared in order to determine the porosity of the specimens and to check whether the found dimples on the fracture surface are formed from plastically deformed pores during testing. In addition, it will be examined to what extent the porosity is related to the scattering of the impact energy and whether the expected impact energy can be derived by determining the porosity. Conclusions are also being drawn about the impact energy as a function of porosity and build-up direction. Further fracture mechanics tests, including the testing of the additively manufactured CT samples, are currently being carried out. The results of the ongoing tests will be presented at SMiRT 2024.

ACKNOLEDGEMENT

This research work is funded in the framework of the German reactor safety research program by the Federal Ministry for Environment, Nature Conservation, Nuclear Safety and Consumer Protection (BMUV) under contract No. 1501644. The support is gratefully acknowledged.

Supported by:

Federal Ministry
for the Environment, Nature Conservation,
Nuclear Safety and Consumer Protection

based on a decision of
the German Bundestag

REFERENCES

Beckers, D. (2019). *"Rapid qualification of new alloys for Additive Manufacturing through a holistic process chain,"* Metal AM Vol. 5 No. 2

Beremin: A. (1983). *"Local Criterion for Cleavage Fracture of a Nuclear Pressure Vessel Steel,"* Metallurgical Transactions A, No. 14A, pp. 2277-2287.

Doel 3 Reactor Pressure Vessel Assessment, Safety Case Report, Electrabel GDF Suez, 5.12.2012.

Jiang, P.F.; Zhang, C.H.; Zhang, S.; Zhang, J.B.; Chen, J.; Chen, H.T. (2021). *"Additive manufacturing of novel ferritic stainless steel by selective laser melting: Role of laser scanning speed on the formability, microstructure and properties*", Optics & Laser Technology, Volume 140, 202

Lacroix, V., Dulieu, P., Bogaert, A. (2015). "*Alternative characterization rules for quasi-laminar flaws based on 3D X-FEM calculations*," Proceedings of ASME Pressure Vessels & Piping conference (PVP 2015), PVP2015-45792, Boston, USA.

Mally, L.; Werz, M.; Weihe, S. (2022). *Feasibility Study on Additive Manufacturing of Ferritic Steels to Meet Mechanical Properties of Safety Relevant Forged Parts*. *Materials* 2022, *15*, 383.

Rousselier, G. (1987). "*Ductile Fracture Models and their Potential in Local Approach of Fracture," Nuclear Engineering and Design*, Volume 105, pp. 97-111.

BMUV-Research project 1501596A. "*Experimental and numerical investigations on crack fields in pressurized components, Phase 2 (MeKomII)"*

BMUV-Research project 1501644. "*Optimization and quality assurance of SLM-manufactured components for nuclear applications (OSKO)"*

Stumpfrock, L, et al. (2022). *"Investigations on the Failure Behaviour of Specimens containing Crack Fields made by Additive Manufacturing",* Proceedings of ASME 2022, USA

Hofer, G.; Hung, C.; Grünes, U. (2022). *"Eine mathematische Funktion für die Beschreibung der Ergebnisse aus Kerbschlagbiegeversuchen";* Werkstofftechnik, 1977; S. 109 – 111

Seebich, H.-P.; Roos, E.; Eisele, U.; Lammert, R.; Restemeyer, D.; Schuler, X.; Seidenfuß, M.; Silcher, H.; Stumpfrock, L. (2006). "*Kritische Überprüfung des Masterkurve-Ansatzes im Hinblick auf die Anwendung bei deutschen Kernkraftwerken";* Abschlussbericht, Vorhaben Nr. 1501 240

Seidenfuß, M. (2014). *"Schädigungsmechanische Modelle zur Beschreibung des Versagensablaufs in metallischen Bauteilen,"* Technical Report, MPA University of Stuttgart.

Sridharan, N.; Gussev, M.; Field, K. (2019). *"Performance of a ferritic/martensitic steel for nuclear reactor applications fabricated using additive manufacturing"*; Journal of Nuclear Materials, Volume 521

Tihange 2 Reactor Pressure Vessel Assessment, Safety Case Report, Electrabel GDF Suez, 5.12.2012

Ty, A.; Mokhtari. M; Balcaen, M., Votié, A.; Cloué, J.-M.; Alexis, J. (2023). "*Performance evaluation of Charpy impact tests to investigate and detect process defects of a Ni-based superalloy elaborated by laser powder bed fusion"*, Journal of Materials Research and Technology, Volume 25